Journal of Polymers and the Environment (2026) 34:182
https://doi.org/10.1007/s10924-026-03901-8

ORIGINAL PAPER

UV-Blocking Active Bioplastics from Coffee Parchment and Pectin

Leticia B. Santos[1,2] · Martina Nardi[2] · Roberto Simonutti[3] · Caio G. Otoni[4,5] · Giovanni Perotto[2] · Athanassia Athanassiou[2] · Henriette M. C. Azeredo[6]

Received: 23 February 2026 / Accepted: 15 June 2026

Abstract

The coffee industry generates large amounts of by-products whose improper disposal may create environmental burdens, while their lignocellulosic matrix and bioactive compounds make them attractive feedstocks for sustainable materials. In this study, coffee husk, parchment, and silverskin were comparatively characterized to identify the most promising fraction for direct conversion into active bioplastics. Based on its composition and film-forming potential, coffee parchment was selected and combined with high-methoxyl pectin to produce films using the biomass in its whole form after mild citric acid pretreatment. The resulting materials were evaluated for mechanical, optical, and functional properties, as well as thermoformability and performance in walnut protection against photooxidative degradation. Depending on formulation, the films showed tensile strength of 3.2–11 MPa, and elongation at break of 30–43%, while all formulations exhibited complete UV-blocking capacity and DPPH radical inhibition of 20–35%. The films could also be thermoformed into three-dimensional structures. In a proof-of-concept application, walnuts packed in the developed films showed markedly lower losses of unsaturated proton signals after UV exposure than walnuts packed in LDPE. These results demonstrate that coffee parchment can act as a main structural component in active bioplastics, supporting whole-biomass valorization for protective packaging applications.

Highlights

- Coffee parchment-based films combine UV-blocking, antioxidant activity, and thermoformability.
- Antioxidant functionality demonstrated by DPPH radical scavenging activity.
- Complete UV-blocking capacity enabling protection against photooxidative degradation.
- Good thermoformability allows processing into a three-dimensional molded structure.
- Sustainable material design supports circular economy strategies for coffee residues.

Keywords Upcycling · Biorefinery · Coffee processing by-products · Active packaging · Coffee parchment

✉ Giovanni Perotto
giovanni.perotto@unipv.it

✉ Henriette M. C. Azeredo
henriette.azeredo@embrapa.br

[1] Graduate Program in Food, Nutrition and Food Engineering, UNESP – São Paulo State University, Rodovia Araraquara-Jaú, Km 01, Araraquara, SP 14800-903, Brazil

[2] Smart Materials, Istituto Italiano Di Tecnologia (IIT), Via Morego 30, 16163 Genoa, Italy

[3] Dipartimento Di Scienza Dei Materiali, Università Di Milano-Bicocca, Via Roberto Cozzi 55, 20125 Milano, Italy

[4] Institute of Chemistry, University of Campinas (UNICAMP), Rua Monteiro Lobato 270, Campinas, SP 13083-862, Brazil

[5] Graduate Program in Materials Science and Engineering (PPGCEM), Federal University of São Carlos (UFSCar), Rod. Washington Luís, Km 235, São Carlos, SP 13565-905, Brazil

[6] Embrapa Instrumentation, R. 15 de Novembro, 1452, São Carlos, SP 13560-970, Brazil

Published online: 03 July 2026

Introduction

Plastic waste generation has increased steadily in recent decades, driven by population growth, urbanization, and the prevailing linear take-make-dispose model associated with single-use plastic products [1]. Under a business-as-usual scenario, plastic waste accumulated in the environment is projected to reach around 12 billion tons by 2050 [2, 3]. In response to the environmental burden posed by persistent plastics and the depletion of fossil resources, significant efforts have been devoted to developing sustainable, bio-based alternatives. In this context, biodegradable materials obtained through the upcycling of agro-industrial residues have emerged as a potential strategy for partially replacing conventional plastics in selected applications [4, 5]. Studies have demonstrated that food processing by-products can be converted into value-added products [5–7], including antioxidant and UV-blocking films derived from orange [8] and banana [9] processing by-products, mechanically robust films from vegetable side streams [10], biocomposite mulch films from spinach stems and orange peels [11], and foldable films from carrot pomace [12].

Different approaches can be used to obtain bio-based films from fruit and vegetable by-products [7, 13–15]. The most common approach involves isolating specific compounds or fractions and using them in film-forming formulations. For example, films have been made from starch, fat, and phenolic compounds extracted from mango kernels [16]. Also, films were made from pectin and cellulose nanocrystals isolated from banana peels [17] and from hemicelluloses and cellulose from wheat straw [18]. A more straightforward approach to producing this type of material is to fully convert the by-products into biocomposites, as demonstrated in previous work [10, 12, 14]. This approach yields higher returns, shorter processing times, reduced waste generation, and minimal use of harsh chemicals. The presence of natural compounds with active properties (e.g., phenolics, essential oils) in those biomasses may contribute to the development of bio-based materials exhibiting antioxidant, antimicrobial, and UV-absorbing properties [19, 20], thereby enabling functional performance in a range of industrial protective material applications.

The coffee industry is one of the largest in the global food sector. According to the International Coffee Organization (ICO), world coffee production in 2023/24 totaled 178 million bags, corresponding to 10.7 million tons of coffee. Coffee cherry processing into coffee beans yields a variety of by-products, namely: pulp, mucilage, parchment, husks, silverskin, and spent coffee grounds, each with distinct chemical compositions and potential for diverse applications. Powdered by-products, for instance, have been used as functional additives in both conventional [21–26] and biodegradable [27–31] plastics. These by-products have also been used as sources of film-forming and/or functional compounds to produce biodegradable materials [32–35].

Recent studies have further highlighted the potential of coffee by-products for packaging applications [19, 20, 36]. For instance, coffee silverskin-derived cellulose has been used to produce composite films for food packaging, including systems containing natural pigments [37]. In addition, recent review literature has summarized the development of biodegradable and compostable packaging materials from coffee residues, including coffee flour, mucilage, husk, silverskin, and spent coffee grounds [38]. Another study has explored coffee silverskin as a component of PLA-based biocomposites for food packaging applications [39]. However, these approaches have mainly focused on silverskin, isolated fractions such as cellulose, or the use of coffee residues as secondary components in pre-existing polymer matrices. In contrast, coffee parchment remains comparatively underexplored as a whole feedstock for active packaging materials, despite its lignocellulosic structure, pectin-related polysaccharides, and intrinsic bioactive compounds, which may contribute to both structural and functional performance.

Materials and Methods

By-Products

Three coffee processing by-products (namely, husk, parchment, and silverskin) were donated by the Federal Institute of Education, Science and Technology of Minas Gerais (IFSULDEMINAS, Campus Machado, MG), Brazil. They were stored in plastic bags away from light before use.

Biomass Characterization

Biomass Composition by Solid-State NMR

The samples were analyzed using solid-state ^{13}C NMR on a Bruker Avance III system, which operates at a Larmor frequency of 400.13 MHz for ^{1}H. Spectra were obtained under Magic Angle Spinning (MAS) at a spinning rate of 10 kHz. Two pulse sequences were used for the measurements: ^{13}C single-pulse excitation with proton high-power decoupling (HPDEC), and ^{13}C-{^{1}H} cross-polarization (CP).

Extractives

Extractives were quantified according to a method reported elsewhere [42] with some adaptations. In this section, only the water-extractable non-structural fraction of the

extractives was quantified. Briefly, 1 g of each dried biomass was suspended in 30 mL of water and put in an ultrasonic bath at 40 kHz for 120 min at 20 °C. After extraction, the suspensions were centrifuged at 5283 x g for 10 min (A5b rotor; Centrisart® G-16C, Sartorius, Germany) and then filtered through a qualitative filter paper. The liquid fraction was used to determine total phenolics, free sugars, and antioxidant activity. The solid part was collected on a previously dried and weighed filter paper. The system was then dried at 50 °C until constant weight, and the extractive content was determined as follows:

$$Direct\,extractives\,(\%) = \left(\frac{m_s - m_{fp}}{m_b}\right) \times 100 \qquad (1)$$

where:m_s = mass of the extractive-free biomass and the filter paperm_{fp} = mass of the dried filter paperm_b = mass of the by-product. In the present study, the directly measured extractable fraction obtained by aqueous ultrasound-assisted extraction included all water-extractable, non-structural components of the biomass. Since pectin and reducing sugars were quantified separately, their values were subtracted from the direct extractives fraction in order to estimate the remaining extractives , thus avoiding double counting. Therefore, the extractives values were calculated as: Extractives = direct extractives − reducing sugars − pectin. The corresponding standard deviations were obtained by error propagation.

Pectin Determination

Pectin percentage was determined using a modified version of a previously described method [43]. Briefly, 2 g of each biomass was suspended in 20 mL of 0.05 M HCl solution. The suspension was heated in a water bath at 100 °C for 1 h and then filtered. The solid residue retained on the filter paper was subjected to a second extraction under the same conditions. The resulting filtrates were combined, and pectin was precipitated by adding two volumes of 95 vol.% ethanol acidified with 0.05 M HCl. The precipitated pectin was then recovered by filtration onto a previously weighed filter paper. The retained pectin was washed with 65 vol.% ethanol, acidified with 0.05 M HCl and dried at 50 °C until constant weight. The dried system was weighed again, and the pectin content was determined as follows:

$$Pectin\,(\%) = \frac{m_{dp} - m_p}{m_b} x100 \qquad (2)$$

where:m_{dp} = mass of the dried pectin and the filter paperm_p = mass of the dried filter paperm_b = mass of the byproduct

Total Reducing Sugars (TRS) and Total Phenolic Compounds (TPC)

TRS content was quantified by the 3,5-dinitrosalicylic acid (DNS) method [44, 45]. Briefly, sample extracts were reacted with DNS reagent, heated in a boiling water bath for 5 min, cooled to room temperature, diluted with deionized water, and their absorbance was measured at 540 nm. CP and CH extracts were diluted sevenfold before analysis. Quantification was performed using a glucose calibration curve (0.1–1.0 g/L). All measurements were carried out in triplicate, and the results are expressed as mean ± standard deviation, as g glucose equivalents per liter (g/L).

TPC was assessed using the Folin–Ciocalteu (FC) colorimetric procedure [46]. Briefly, sample extracts were mixed with Folin–Ciocalteu reagent and sodium carbonate solution, and the reaction mixtures were kept at 22 °C for 2 h. Absorbance was then measured at 760 nm. Gallic acid was used as the external standard for calibration. Analyses were performed in triplicate, and results are expressed as mean ± standard deviation, as mg gallic acid equivalents per 100 mL.

Antioxidant Assays

The antioxidant assays were done following the 2,2-diphenyl-1-picryl-hydrazyl-hydrate (DPPH) free radical method [47] and the 2,2'-Azino-bis(3-ethylbenzothiazoline-6-sulfonic acid) diammonium salt radical cation (ABTS•+) method [48].

A DPPH working solution in ethanol was prepared from a stock solution and kept protected from light. Trolox in ethanol (50–1000 µM) was used for the calibration curve. For the assay, 150 µL of each standard or sample extract was mixed with 5.850 mL of DPPH working solution, and the mixtures were kept in the dark for 15 min. Absorbance was then measured at 515 nm, using ethanol as the blank. Analyses were performed in triplicate, and results are expressed as mean ± standard deviation in Trolox equivalents.

The $ABTS^{\cdot+}$ radical cation was generated by reacting ABTS stock solution (7 mM) with potassium persulfate solution (140 mM) and keeping the mixture in the dark at room temperature for 16 h. Before analysis, the radical solution was diluted with ethanol to an absorbance of 0.70 ± 0.05 at 734 nm. A 2 mM Trolox solution in ethanol was used to prepare the calibration curve (50–2000 µM). For the assay, 30 µL of each standard or sample extract was mixed with 3.0 mL of diluted ABTS radical solution, and the absorbance was measured at 734 nm after 6 min, using ethanol as the blank. Analyses were performed in triplicate, and results were expressed as mean ± standard deviation in Trolox equivalents.

Thermal Properties

Thermogravimetric analysis (TGA) was performed on a Q500 instrument (TA Instruments) using sample masses of 15-30 mg. Measurements were conducted under a nitrogen atmosphere (50 mL/min). The temperature program ranged from 30 to 800 °C, with a constant heating rate of 10 °C/min. Throughout the run, sample mass loss and its first derivative (DTG) were recorded as functions of temperature and time. Mass loss values were expressed relative to the initial mass at 30 °C. The final residual mass at 800 °C was taken as an estimate of the ash content of each biomass. Since one TGA run was performed for each biomass fraction, ash values are reported as single values, and no standard deviation is provided for this parameter.

Film Preparation

Coffee parchment (CP) and a commercial high-methoxyl pectin (HMP; Aglupectin HS-SP, Silva Extracts S.r.l.) were used as received. The choice of high-methoxyl pectin was based on the FTIR profile of pectin preliminarily extracted from coffee parchment, which suggested a high-methoxyl character. According to the manufacturer, the degree of methoxylation of the commercial pectin is in the 58–67% range. Both powders were combined at weight ratios of 100:0, 90:10, 80:20, 70:30, and 60:40 (CP:HMP). For each formulation, 1 g of solids was dispersed in 15 mL of 0.1 M citric acid solution and magnetically stirred at 40 °C for 12 h to obtain a viscous dispersion. The resulting dispersions were cast onto square 12 cm x 12 cm Petri dishes lined with a previously cured PDMS substrate. Films were dried in a fume hood at room temperature (approximately 25 °C) and then left uncovered for at least 48 h. At least three films were prepared for each formulation.

Film Characterization

Film Thickness

Film thicknesses were measured before thermoforming using a digital micrometer at least five different positions of each film.

Scanning Electron Microscopy (SEM)

SEM was employed to examine the film surface after it was mounted on a metallic stub using carbon tape and then sputter-coated with a 15 nm gold layer. Imaging was performed on a JEOL JSM-6490LA Scanning Electron Microscope, utilizing a secondary electron detector and an acceleration voltage of 5 kV.

Fourier-Transform Infrared (FTIR) Spectroscopy

FTIR measurements were performed using a Vertex 70v Bruker spectrophotometer equipped with Attenuated Total Reflectance (ATR) mode, utilizing an accessory fitted with a diamond crystal. The measurements were acquired with 64 scans over the range of 4000–600 cm^{-1} at a spectral resolution of 4 cm^{-1}.

Thermal Stability

TGA was carried out using a Q500 TGA (TA Instruments) on film samples of about 1 cm^2. The analysis was conducted under an inert nitrogen atmosphere with a flow rate of 50 mL/min. The temperature was ramped from 30 to 800 °C at 10 °C/min. The mass loss data were normalized to the initial mass at 30 °C.

Mechanical Properties

Mechanical properties were evaluated using uniaxial tensile testing on an INSTRON 3365 universal testing machine at a crosshead speed of 10 mm/min. Samples were cut into a dog-bone geometry, with the gauge section measuring 25.01 mm in length and 3.98 mm in width. Prior to testing, the specimens were equilibrated for at least 24 h in an Espec SH-262 environmental chamber set to 50% relative humidity and 25 °C. A minimum of five replicates per film type was tested. Young's modulus (E), tensile strength (σ), and elongation at break (ε) were derived from the resulting stress (MPa)–strain (mm/mm) curves, and data are expressed as mean ± standard deviation.

X-Ray Diffraction (XRD)

XRD measurements were conducted using a PANalytical Empyrean diffractometer equipped with a 1.8 kW copper Kα ceramic X-ray tube and a PIXcel3D 2 × 2 area detector, operating at 45 kV and 40 mA. The diffraction data were acquired in Parallel-Beam geometry and symmetric reflection mode on a zero-diffraction silicon substrate. The angular range for data collection was set from 2θ = 5° to 80°, with a step increment of 0.026°.

UV–Visible (UV–Vis) Spectroscopy

UV-Vis spectra were recorded in quintuplicate for each formulation in a Cary 6000i UV-Vis-NIR spectrophotometer (Varian Inc.), equipped with a film holder. UV-shielding percentages (SUV) were determined using equations 3-5 for the three wavelength regions of the UV (UVA: between

320 and 400 nm; UVB: between 280 and 320 nm; and UVC: between 200 and 280 nm).

$$S_{UVA}\,(\%) = 100 - T_{UVA} = 100 - \frac{\sum_{320}^{400} T_\lambda x \Delta\lambda}{\sum_{320}^{400} \Delta\lambda} \quad (3)$$

$$S_{UVB}\,(\%) = 100 - T_{UVB} = 100 - \frac{\sum_{280}^{320} T_\lambda x \Delta\lambda}{\sum_{280}^{320} \Delta\lambda} \quad (4)$$

$$S_{UVC}\,(\%) = 100 - T_{UVC} = 100 - \frac{\sum_{200}^{280} T_\lambda x \Delta\lambda}{\sum_{200}^{280} \Delta\lambda} \quad (5)$$

with T_{UVA}, T_{UVB} and T_{UVC}

Corresponding to the average transmittance values calculated for the three spectral regions examined. In this expression, λ represents the wavelength, Δλ the width of the wavelength interval, and T_λ the spectral transmittance.

3D Modeling, Mold Printing, and Thermoforming of the Coffee-Pectin Bioplastics

Thermoforming was performed by hot-pressing films between 3D printed PLA molds. The mold sketch was designed in Blender (v 3.6) and then printed in PLA on a 3D printer (Sharebot VIPER).

The molding process was carried out by heating up the mold and the bioplastic in an oven at 55 °C for 5 min. After that, the film was placed in the mold, and a 10 kg load was placed directly on top of the mold assembly during hot pressing. The pressing took place for 5 min, and after that, the system was removed from the oven and left to cool for another 5 min before demolding the trays.

Walnut Packaging

To quantify the UV protection of our materials, we used walnuts purchased at a local supermarket, packaged in LDPE films or in biocomposite films obtained from CP and HMP. Walnut kernels were crushed into small pieces and exposed to UV radiation to induce oxidation. The samples were placed under a UV lamp emitting at a wavelength of 254 nm (Analytik Jena US, USA; 230 V, 50 Hz) at a distance of 15 cm and irradiated continuously for 7 days, following the previously described procedure [49]. The CP-HMP films were used as packaging material to evaluate their protective effect. To seal the films, a small amount of water was applied to the corners of the material, which was then hot-sealed by pressing it onto a hot plate at 100 °C under a 10 kg weight for approximately 1 min.

Oil Extraction from Walnuts Packed with Coffee-Pectin Films

Oils were extracted according to a method described elsewhere with some modifications [50]. Briefly, 1 g of walnuts was collected in triplicate from each treatment, and its oil was extracted with 7.5 mL of ethyl acetate. The system was placed in an ultrasound bath for 15 min at 59 kHz and 20 °C. The filtrate was collected with a Büchner funnel, and the nuts were resuspended twice. All three filtrates were combined and allowed to evaporate on a large Petri dish placed on a hot plate at 40 °C until the ethyl acetate was completely removed. The lipids were collected in amber glass flasks.

Walnut Oil Analysis by ^{1}H NMR

Proton nuclear magnetic resonance (^{1}H NMR) spectra were acquired at room temperature using 5 mm NMR tubes on a Bruker Avance III spectrometer operating at 400 MHz. Chemical shifts are given in ppm and referenced to tetramethylsilane (TMS). Quantitative ^{1}H NMR measurements were obtained using 16 scans (NS = 16) and a relaxation delay of 30 s (D1 = 30 s). The spectra were processed and analyzed with TOPSPIN software. The signal area was normalized to the CH2 signal of the glycerol moiety of triglycerides (4.12-4.31 ppm) corresponding to four protons. The method to evaluate the oxidation of triglyceride double bonds has been described elsewhere [51]. Specifically, the percentage loss (%) after UV irradiation of allylic (δ = 2.02 ppm), bisallylic (δ = 3.74 ppm), and olefinic (δ = 5.34 ppm) protons was calculated according to the following equations:

$$\%Hloss = \frac{oleH\,(0) - oleH(t)}{oleH(0)} x100$$

$$\%Hloss = \frac{allyH\,(0) - allyH\,(t)}{allyH\,(0)} x100$$

$$\%Hloss = \frac{bisalH\,(0) - bisalH(t)}{bisalH(0)} x100$$

Where ole H (0), ally H (0), and bisal H (0) are the integration value of olefinic, allylic, and bisallylic protons, respectively, before UV irradiation and ole H (t), ally H (t) and bisal H (t) are the integration value of olefinic, allylic and bisallylic protons, respectively, after different UV irradiation times. In the case of olefinic protons, the ^{1}H-NMR signal is overlapped with the signal of the C-H proton of the glycerol unit at 5.1 ppm. Therefore, the two different signals were integrated together and then subtracted by the value of 1 to obtain the integration value of the olefinic protons

Table 1 Composition of the coffee by-products of the study, obtained by deconvolution of ^{13}C CPMAS NMR spectra using the methodology described in the experimental section

Component (mol %)	Coffee by-product		
	Husk	**Parchment**	**Silverskin**
Cellulose	25.40	27.50	36.40
Pectin	28.80	33.80	28.00
Hemicellulose	19.50	21.30	15.80
Lignin	22.80	15.70	18.40
Polyesters	3.500	1.700	1.400
Sum	100.0	100.0	100.0

alone. The final % H loss was calculated on the average of three measurements.

Results and Discussion

Biomass Characterization

The three coffee by-products were characterized by complementary structural and chemical approaches. The relative distribution of the main lignocellulosic components estimated from solid-state ^{13}C NMR is shown in Table 1, whereas the results obtained by chemical methods are presented in Table 2 and discussed in comparison with literature data.

Coffee husks, generated during dry processing, account for approximately 45% of the coffee cherry weight on a dry basis, whereas coffee parchment is obtained through wet processing and represents around 5.8 % of the dry coffee cherry weight [40]. Coffee silverskin, a by-product common to both processing routes, is produced during coffee bean roasting and constitutes about 0.4-4.2% of the coffee cherry dry weight [40, 41]. In this context, the present study first screened three coffee processing by-products, namely coffee husks, parchment, and silverskin, to identify the most suitable fraction for active bioplastic development. Based on this screening, coffee parchment was selected and used in its whole form after mild pretreatment as the main structural component of films combined with high-methoxyl pectin. The resulting materials were evaluated in terms of their structural, mechanical, optical, barrier-related, antioxidant, and thermoforming properties, and their protective performance was further assessed in a proof-of-concept study using walnuts exposed to UV radiation .

The ^{13}C CP-MAS NMR spectra (Supporting Information, Figure S1) indicate that coffee parchment is composed of lignin, cellulose (mostly amorphous), hemicellulose, pectin,

Table 2 Chemical composition of coffee by-products obtained by chemical methods

Component		Byproduct					
		Husk (CH)		**Parchment (CP)**		**Silverskin (CS)**	
Moisture (%)		5.28 ± 0.06^{B}	This work	4.60 ± 0.05^{A}	This work	12.0 ± 0.07^{C}	This work
		2.6–15	[53, 54, 56–59]	6.33	[55]	1.05–8.2	[55, 69–73]
Composition (wt% dry basis)							
Pectin		1.39 ± 0.37^{A}	This work	5.55 ± 0.23^{B}	This work	0.86 ± 0.18^{A}	This work
		1.30–6.58	[53, 74]	-	-	-	-
Ashes*		8.4	This work	5.7	This work	4.8	This work
		0.2–9.5	[53, 54, 56–58, 67, 75–78]	0.65–3.0	[67, 79, 80]	4.7–9.47	[67–71, 73, 81–83]
Extractives**		16.7 ± 0.4	This work	1.4 ± 0.7	This work	13.5 ± 1.1	This work
		6.7–10.8	[75, 78]	3.1–7.0	[79, 80]	15.0	[82]
Free reducing sugars		15.00 ± 0.02^{B}	This work	31.40 ± 0.14^{C}	This work	2.00 ± 0.03^{A}	This work
		12–14	[57, 58, 84]	-	-	0.2–1.07	[69, 71, 72, 83, 85]
Antioxidant	TPC (mg GA / g byproduct)	11.1 ± 0.2^{B}	This work	12.1 ± 0.2^{C}	This work	9.7 ± 0.7^{A}	This work
		2.75–9.83	[53, 86]	2.0	[34]	2.79–20.5	[42, 85, 87–93]
	DPPH (g TE / 100 g byproduct)	0.42 ± 0.01^{C}	This work	0.37 ± 0.02^{B}	This work	0.30 ± 0.02^{A}	This work
		0.29	[67]	0.05	[67]	0.19	[67]
	$TEAC_{ABTS}$ (µmol Trolox/g byproduct)	344 ± 15^{A}	This work	423 ± 21^{A}	This work	379 ± 51^{A}	This work
		755.9	[53]	-	-	598	[68]

Values within the same row followed by at least one common letter or not followed by letters are not significantly different (Tukey's test, $p > 0.05$). *Ash values were estimated from the final residual mass in the TGA curves at 800 °C. Since one TGA measurement was performed for each biomass fraction, these values are reported without standard deviation. **Values obtained by subtracting reducing sugars and pectin values, corresponding to the water-extractable non-structural fraction of the lignocellulosic compounds; standard deviations were obtained by error propagation

and aliphatic polyesters like cutin and suberin. These aliphatic polyesters contribute signals across multiple regions, such as aliphatic carbons (20–40 ppm) and carboxyl groups (~173 ppm), shared with lignin, fatty acids, hemicellulose, and pectin. Key signals include peaks for lignin (OCH_3, 54.5 ppm and aromatic groups 115–160 ppm), cellulose (C1 105 ppm, C4, and ring carbons 60–90 ppm), hemicellulose ($CH_3\boldsymbol{C}OO-$ groups 170 ppm and xylose-based rings), and pectin (galacturonic acid and carboxyl groups 165–175 ppm).

The coffee husk spectrum is similar to that of parchment, but with a significantly lower intensity at 99 ppm, indicating a reduced pectin content compared to parchment. An increased signal from lignin is also present.

The ^{13}C CP-MAS NMR spectrum of coffee silverskin differs notably from parchment and husk, showing higher aliphatic polyester content (peaks at 14.7 ppm and 33.1 ppm), increased lignin (peaks at 55 ppm and 115–160 ppm), and more crystalline cellulose (sharp peaks at 65, 84, 88.5, and 105 ppm). In silverskin, the sharp peak at 99 ppm is significantly reduced, and it disappears under the Lorentzian peak of cellulose anomeric carbon, indicating a reduced contribution from pectin and hemicellulose. This is also confirmed by the lower carbonyl peak intensity. This interpretation is consistent with previous reports on coffee silverskin, in which lignin, cellulose, and hemicellulose were identified by solid-state ^{13}C CP-MAS spectroscopy [52].

While the solid-state NMR analysis was mainly used to compare the structural composition of the three biomasses in terms of their main lignocellulosic components, the chemical analyses provided complementary information on the non-structural and water-extractable fractions, including sugars, pectin, phenolic compounds, and antioxidant activity. These latter components are particularly relevant to the proposed application, since they may contribute to the active and UV-protective properties of the resulting materials.

The levels obtained for the composition of coffee processing by-products are, in general, consistent with those reported by various other authors in the literature (Table 2). These values may vary depending on the coffee variety, processing method, and the extraction techniques used for each compound studied. The moisture content of coffee husk varies with the drying time used by each author [53–59]. The extractive content varies with the method and solvent used, which in turn influences the experimental yield; however, they are usually rich in phenolic compounds, such as caffeic and chlorogenic acids [60]. A high concentration of phenolics is expected to be found especially in the outer parts of the cherry since the primary function of these metabolites is to protect against external threats to the plant [61]. Other bioactive compounds are also present, including rutin, catechin, epicatechin, anthocyanins, and caffeine [62–66]. The antioxidant potential of the compounds found in those plant extracts can vary depending on their structure and concentration in the plant. The studied biomasses showed high antioxidant activity (DPPH: 0.42 ± 0.01, 0.37 ± 0.02, and 0.30 ± 0.02 g TE / 100 g by-product for husk, parchment, and silverskin, respectively), similar to other studies [53, 67, 68].

The pectin values obtained by extraction are corroborated by those found by NMR. Coffee parchment has the highest pectin content (5.5%), followed by coffee husks (1.39%) and silverskin (0.86%).

The SEM micrographs and the inset pictures (Fig. 1, a-c) show the morphology of the coffee husk (CH), parchment (CP), and silverskin (CS) powders. Husk and parchment have similar particle morphologies, characterized by irregular shapes, varying sizes, and rough surfaces, whereas silverskin particles exhibit a well-defined rod shape, with smooth surfaces.

The FTIR spectra of the three coffee by-products (Fig. 1, d) showed prominent bands in the following ranges: 3300, 2930–2850, 1800–1600, and 800–700 cm^{-1}, which are consistent with the presence of typical lignocellulosic components [94]. At 3320 cm^{-1}, the vibration band corresponds to the O–H bonds, which can be assigned to the stretching vibration commonly present in cellulose, hemicellulose, and phenolic compounds. Bands at 2921 and 2847 cm^{-1} correspond to the asymmetric and symmetric C-H stretching vibrations of aliphatic chains, which can originate from lipids, waxes, or polysaccharide structures [95, 96]. Although the extractive content varied among the residues (as shown in Table 2), the presence of these bands in all samples suggests some contribution of aliphatic compounds, possibly enhanced by residual seed particles occasionally found within the by-products, which were ground and included in the samples.

The band at 1735 cm^{-1} is typically assigned to the C=O stretching of ether groups, which may be attributed to hemicellulose acetyl groups, pectins, lipids, or esters [95, 97].

In the 1700 and 1500 cm^{-1} region, overlapping absorptions can arise from C=C and C=N stretching vibrations in aromatic and heterocyclic compounds, including alkaloids such as trigonelline [95, 97, 98]. At 1512 cm^{-1}, the vibration of the aromatic ring in lignin is observed. In the region of 1450–100 cm^{-1}, the corresponding bonds for chlorogenic acids are assigned (C-H, C-O, and C-N). These acids correspond to a family of esters formed between one to four residues of caffeic, *p*-coumaric, and ferulic and quinic acids [99]. Bands in the range of 1450 to 1245 cm^{-1} are assigned to the stretching of acetyl groups present in lignin, corresponding to the C-H and C-O bonds. Several carbohydrate bands can be observed from 1500 to 700 cm^{-1}. Pectic polysaccharides have a peak around 1237 cm^{-1}, corresponding

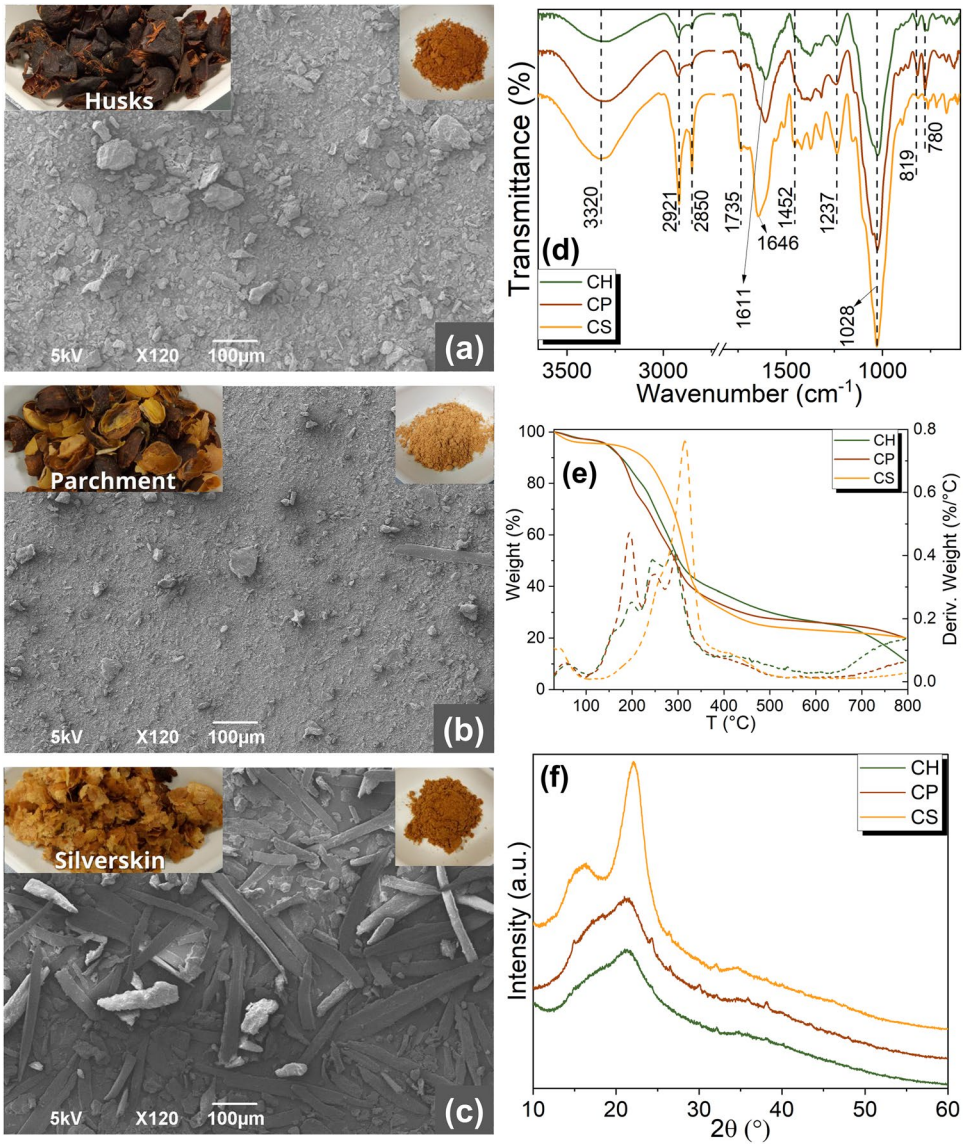

Fig. 1 Coffee by-products used in this study and their SEM micrographs: (**a**) husks, (**b**) parchment, and (**c**) silverskin; (**d**) FTIR of coffee husks (CH), coffee parchment (CP), and coffee silverskin (CS); (**e**) TGA of the different biomasses; (**f**) XRD of the different biomasses

to the bending of O–H groups in the pyranose ring of pectins [100]. At 950–700 cm^{-1}, the bands are associated with the skeletal vibrations and glycosidic linkages of polysaccharides. The peak at 896 cm^{-1} corresponds to the C_1 ring frequency of cellulose [100].

The TG and DTG profiles (Fig. 1e) show similar thermal events across all biomasses studied in this work. The initial weight loss observed between 30–105 °C is primarily attributed to the removal of moisture and low-molecular-weight components. This is followed by a second mass loss stage in the range of 105–220 °C, corresponding to the decomposition of hemicelluloses, with a notable DTG shoulder at 190 °C. The third significant mass loss occurs between 220 and 350 °C, associated with the decomposition of cellulose and a portion of hemicelluloses, with a peak in hemicellulose decomposition at ca. 255 °C. Finally, the last degradation phase, occurring between 350 and 650 °C, is attributed to the decomposition of lignin, with a substantial weight loss observed above 400 °C.

The XRD diffractograms of the powders show similar characteristics (Fig. 1f). All samples exhibit the three characteristic diffraction peaks (2θ = 14.7, 16.2, and 22°) of cellulose crystalline planes [90–94]. Coffee husks and parchment show a lower intensity in this region, while silverskin has more intense peaks, suggesting that a significant portion of its cellulose is crystalline, as corroborated by NMR.

Biocomposite Films

Biocomposite films were fabricated according to the procedure summarized in Fig. 2 [10, 12, 14], using all three biomasses studied here. Films made from 100% biomass showed poor results, with uneven shape and brittleness (Figure S2, Supporting Information). The comparative

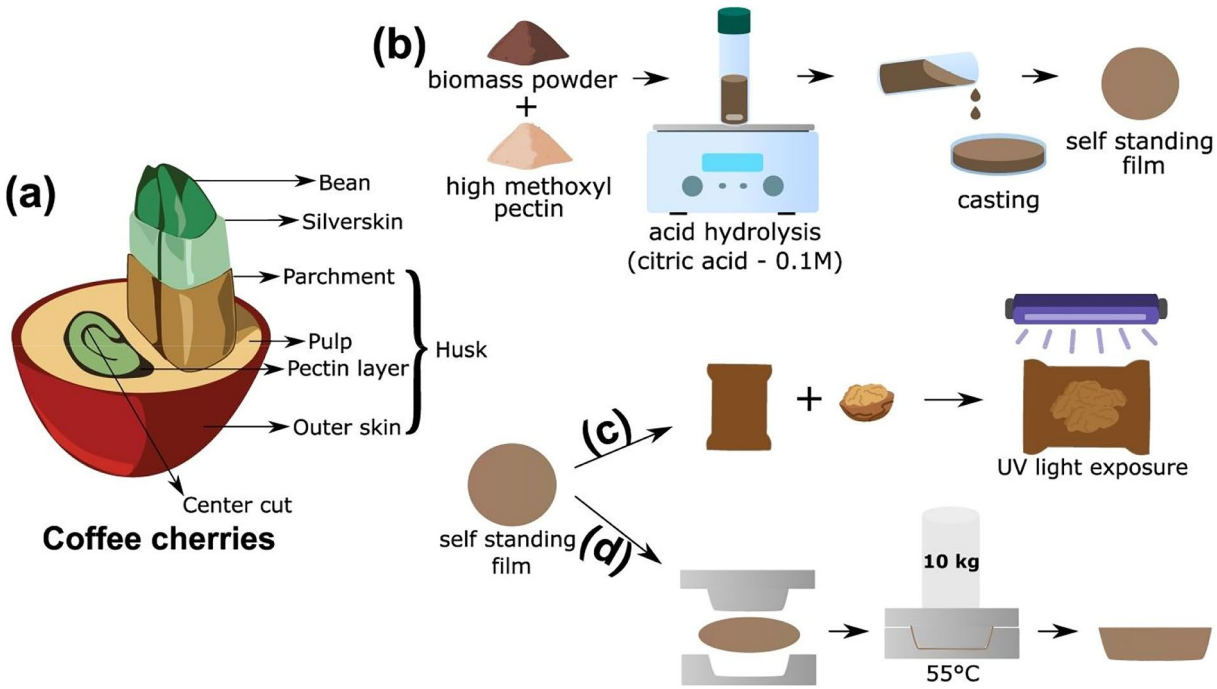

Fig. 2 (**a**) Coffee cherry anatomy; (**b**) coffee-pectin bioplastic fabrication process; (**c**) scheme of the walnut oxidation experiment; (**d**) thermoforming process to produce trays

Table 3 Properties of films based on coffee parchment and pectin in different proportions

Property	Formulation			
	90CP:10HMP	**80CP:20HMP**	**70CP:30HMP**	**60CP:40HMP**
Thickness (mm)	0.19 ± 0.01^{a}	0.19 ± 0.03^{a}	0.20 ± 0.04^{a}	0.17 ± 0.01^{a}
ε (%)	38 ± 1^{c}	43 ± 2^{b}	31 ± 4^{a}	30 ± 2^{a}
E (MPa)	66 ± 9^{a}	53 ± 6^{a}	179 ± 10^{b}	298 ± 61^{c}
σ (MPa)	3.2 ± 0.2^{a}	5.7 ± 0.5^{b}	11 ± 1^{c}	10 ± 1^{c}
TVis (%)	1.1 ± 0.14^{a}	1.4 ± 0.3^{a}	3.2 ± 0.4^{b}	3.7 ± 0.4^{b}
S_{UVA} (%)	100	100	100	100
S_{UVB} (%)	100	100	100	100
S_{UVC} (%)	100	100	100	100
% Inhibition DPPH radical	35 ± 1^{c}	$31 \pm 2^{b,c}$	28 ± 1^{b}	20 ± 1^{a}

ε: elongation at break; E: elastic modulus; σ: tensile strength; T_{vis}: transparency of the films. Values within the same row followed by at least one common letter or not followed by letters are not significantly different (Tukey's test, $p > 0.05$).

characterization of husk, parchment, and silverskin was used as a screening step to identify the most suitable coffee by-product for direct conversion into bio-based films. Among the three fractions, coffee parchment showed the highest potential, primarily because of its higher contents of pectin and reducing sugars, the latter plasticizing the film. In a previous study, we showed how pectin provides flexibility in these plant-based biocomposite films, while solid lignin and crystalline cellulose provide mechanical strength [10]. Consequently, only CP was selected for packaging material development. CP biomass was mixed with different proportions of HMP. Four formulations were developed to evaluate the influence of component concentration on the properties of the resulting films and to identify the most suitable compositions for bio-based protective material applications, using different CP:HMP ratios (90:10, 80:20, 70:30, and 60:40).

The films produced from the combination of coffee parchment and pectin were cohesive and homogeneous across all four formulations (Figure S3a, Supporting Information) and were to some extent transparent (Table 3).

They all exhibited a brownish color, owing to phenolic-rich extracts obtained from coffee by-products [41]. All SEM micrographs (Fig. 3) indicate rough surfaces due to the heterogeneous composition and structure of the coffee parchment. The cross-sectional images do not evidence phase separation between pectin and CP, indicating a proper interaction among all components.

The infrared spectra (Figure S3a, Supporting Information) of the coffee-pectin films presented the typical bands associated with carbohydrates of the plant cell wall [100] as

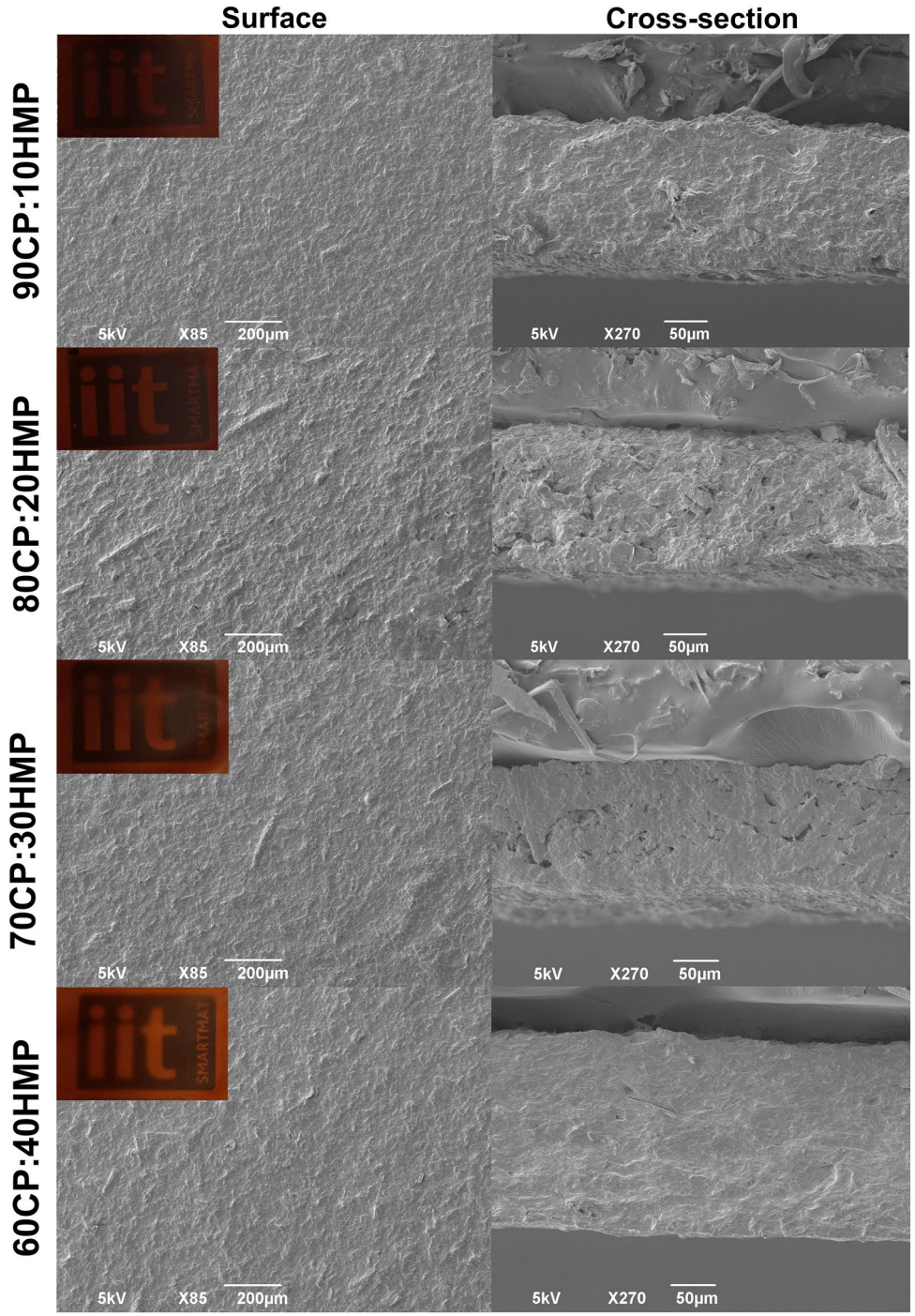

Fig. 3 Visual aspects, surface and cross-sectional SEM micrographs of the films

indicated in the isolated biomass spectra (Fig. 1, d). Vibrations associated with chemical groups present in pectin are evident as well, such as the one in 2936 cm^{-1}, corresponding to -CH, CH_2, and $-CH_3$ stretching from methyl esters of galacturonic acid [101]. Vibrations at 1717 cm^{-1}, corresponding to C=O stretching and at 1640 cm^{-1} COO^-, assigned to stretching from pectin, are present. The coexistence of these bands indicates the presence of both coffee parchment- and pectin-related structures within the film matrix. The retention of characteristic absorptions from both components after film formation suggests successful incorporation of HMP into the parchment-based system. Although no new absorption bands were observed, the spectral profile is consistent with the occurrence of intermolecular interactions, most likely hydrogen bonding, rather than the formation of new covalent bonds detectable by FTIR.

Regarding the XRD of the films (Figure S3b, Supporting Information), the most evident peaks in the diffractograms

refer to pectin (16.3° and 21.7°) [102], which overlap with the peaks corresponding to cellulose and other components, making it difficult to highlight them.

The films comprising lower CP contents (60CP:40HMP and 70CP:30HMP) showed the highest elastic modulus values (Fig. 4a, Table 3), which could be attributed to the positive interaction between pectin and CP and the polyphenolic compounds present in the CP. The polyphenolic compounds may have interacted with pectin chains by being incorporated with the polymer chains of pectin, enhancing molecular interactions through the formation of hydrogen bonds and possibly covalent bonds with reactive groups of pectin (not demonstrated). Although no direct evidence was obtained in this study, previous studies have proposed such interactions in plant-based matrices, particularly in systems rich in phenolic acids and pectic substances [103, 104]. In a previous study on orange processing by-products, films produced from orange peel and orange pomace—fractions known to be richer in pectin—showed elastic modulus values similar to those observed in the formulation with the highest pectin content from the present work [8]. The 70CP:30HMP formulation exhibited an elastic modulus similar to the combination film of the three orange by-products studied (peel, pomace, and pulp) and comparable to films made from parsley stems [10]. The two formulations with higher CP content exhibited lower elastic moduli, which may be attributed to the higher content of small components such as sugars. This could lead to discontinuities in the polymer matrix, and possibly the lower pectin content was insufficient to act as a binder for the different biomass fractions or to form a significant number of hydrogen bonds with them. The elongation at break was similar across all four compositions and was consistent with previous results for carrot and orange biomass [10, 12, 14]. The formulation 80CP:20HMP showed slightly higher elongation, despite containing less sugar than 90CP:10HMP, which may be attributed to the higher pectin content acting as an efficient binder and compensating for the lower plasticization. Since sugars act as plasticizers, they promote the mobility of polymer chains relative to one another, contributing to the elongation of the materials. Similar behavior has been reported in pectin films, where sufficient pectin is required to form a continuous, cohesive matrix, while sugars and other plasticizers primarily contribute to chain mobility and flexibility [105]. Furthermore, studies optimizing pectin-plasticizer ratios have highlighted that only at intermediate compositions the polymer acts effectively as a binder, whereas excessive plasticization without adequate pectin content results in weak

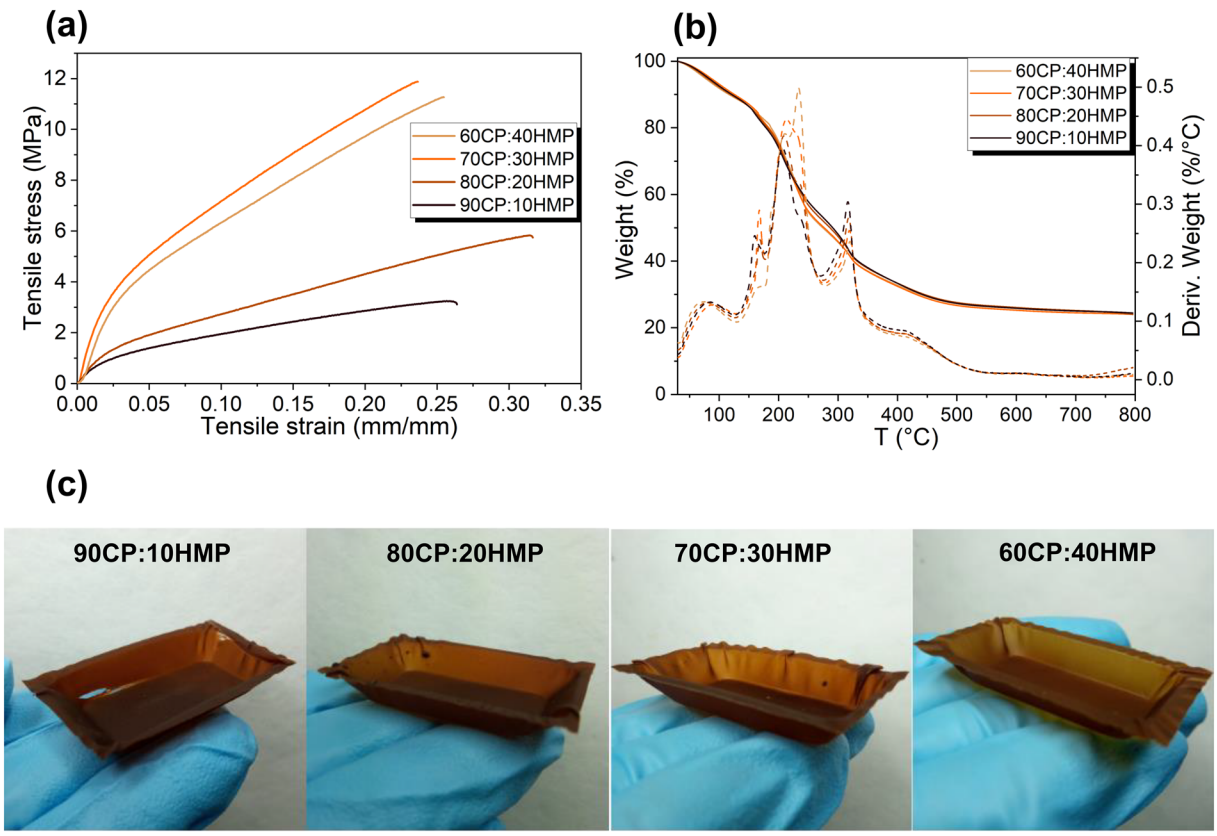

Fig. 4 (**a**) Tensile properties and (**b**) TG profiles of films with different coffee parchment (CP): high-methoxyl pectin (HMP) ratios; (**c**) thermoformed coffee-pectin film trays from different CP:HMP ratios

and fragile films [106]. Regarding tensile strength, values increase with increasing HMP content in the film formulation, possibly due to higher sample homogeneity, with pectin acting as an efficient binder. Compared with films from other biomasses, such as rice husks, spinach, and parsley stems [101], the coffee pectin films exhibit higher tensile strength. The films with higher pectin content showed tensile strengths similar to those of banana peel powder films combined with carboxymethylcellulose (CMC) [9].

Since film thickness did not differ significantly among formulations, the variations observed in mechanical, optical, and antioxidant properties can be primarily attributed to changes in the CP:HMP ratio rather than to geometric effects. Overall, the data in Table 3 reveal composition-dependent changes in film performance: increasing the HMP content improved stiffness and tensile strength, whereas increasing the CP content reduced transparency and increased radical scavenging activity. While lower transparency may be disadvantageous in applications requiring product visibility, it can be beneficial for the protection of light-sensitive products. Importantly, all formulations retained complete UV-blocking capacity, indicating that compositional adjustments can be used to tune the mechanical profile of the films without compromising this key protective property. Among the tested compositions, the 70CP:30HMP formulation provided the most balanced combination of tensile strength, stiffness, antioxidant activity, and UV-shielding performance.

The TG analysis for all coffee-pectin films showed similar degradation pathways, suggesting that changing the CP:HMP ratio did not substantially alter the thermal decomposition behavior of the matrix (Fig. 4, b). The first stage is around 85 and 160 °C and corresponds to the desorption of volatile compounds and moisture. The third and fourth stages observed at 175–255 and 280–385 °C correspond to hemicellulose and pectin decomposition [102]; cellulose, a part of hemicelluloses, and some contributions of pectin, respectively. Cellulose decomposition was observed in the range of 385–460 °C [95], while lignin begins to decompose at temperatures up to 650 °C. The residual mass corresponds to ashes [107]. These data also indicate that the films are thermally stable under the thermoforming conditions used (55 °C), since degradation starts at much higher temperatures.

The coffee-pectin films were successfully thermoformed into $30 \times 13 \times 6$ mm^3 trays using a 3D-printed PLA mold by hot-pressing (see Supporting Information, Figure S4). The working temperature was 55 °C, to stay below the Tg of PLA (~60–65 °C), and preserve its dimensional stability. Samples were pressed for 1 to 5 min; the latter being chosen for further tests.

As can be seen in Fig. 4c, materials with the highest CP content (90CP:10HMP) exhibited some tearing, attributed to their inferior tensile properties, particularly tensile strength. All trays started to show a gradual deformation some minutes after pressing, trending toward a flattened structure. The observed loss of shape and flattening of the structure are attributed to the mild processing conditions. While higher pressing temperatures could improve chain mobility, rearrangement, and flowability, such conditions were not applied due to the thermal limitations of the PLA mold. Future work using molds resistant to higher temperatures could explore this possibility in order to improve structural retention. Despite these limitations, the ability to thermoform the materials—even under mild conditions—underscores their potential for applications that require more intricate three-dimensional geometries in bio-based protective materials.

Applicability: Functional Properties of Coffee-Pectin Bioplastics and Oxidative Stability of Walnuts

Regarding the functional performance of sustainable bio-based materials, the ability to act as a UV barrier is highly desirable. Such a property enables materials to mitigate photoinduced degradation processes, thereby helping to preserve the integrity of light-sensitive products and extend their functional lifespan [108]. Both the transparency and the interaction of the films with UV light were evaluated, as shown in Fig. 5a.

The two formulations with lower CP content (60CP:40HMP and 70CP:30HMP) exhibited higher transparency (3.70% and 3.25%, respectively; Fig. 3 and Table 3) than the other two formulations with higher CP content. Although transparency may be desirable in some applications, increased opacity can be beneficial for materials intended to shield light-sensitive products from photoinduced degradation. The opacity of the studied formulations increases with increasing CP content, thereby increasing the concentration of phenolic compounds as well. Films made from carboxymethylcellulose and enriched with spent coffee ground extracts showed an increase in opacity as the percentage of coffee extract increased in the formulations [109].

All films show very high UV-absorption capacities (100.0%) (Fig. 5a, and Table 3), which can be attributed to the high concentration of phenolic compounds naturally present in the coffee biomass. This functional characteristic makes the materials particularly suitable for applications requiring effective protection against photooxidative degradation, especially when compared with conventional light-permeable polymeric materials (Fig. 5a). In addition, the films exhibited good antioxidant activity (Fig. 5b), further

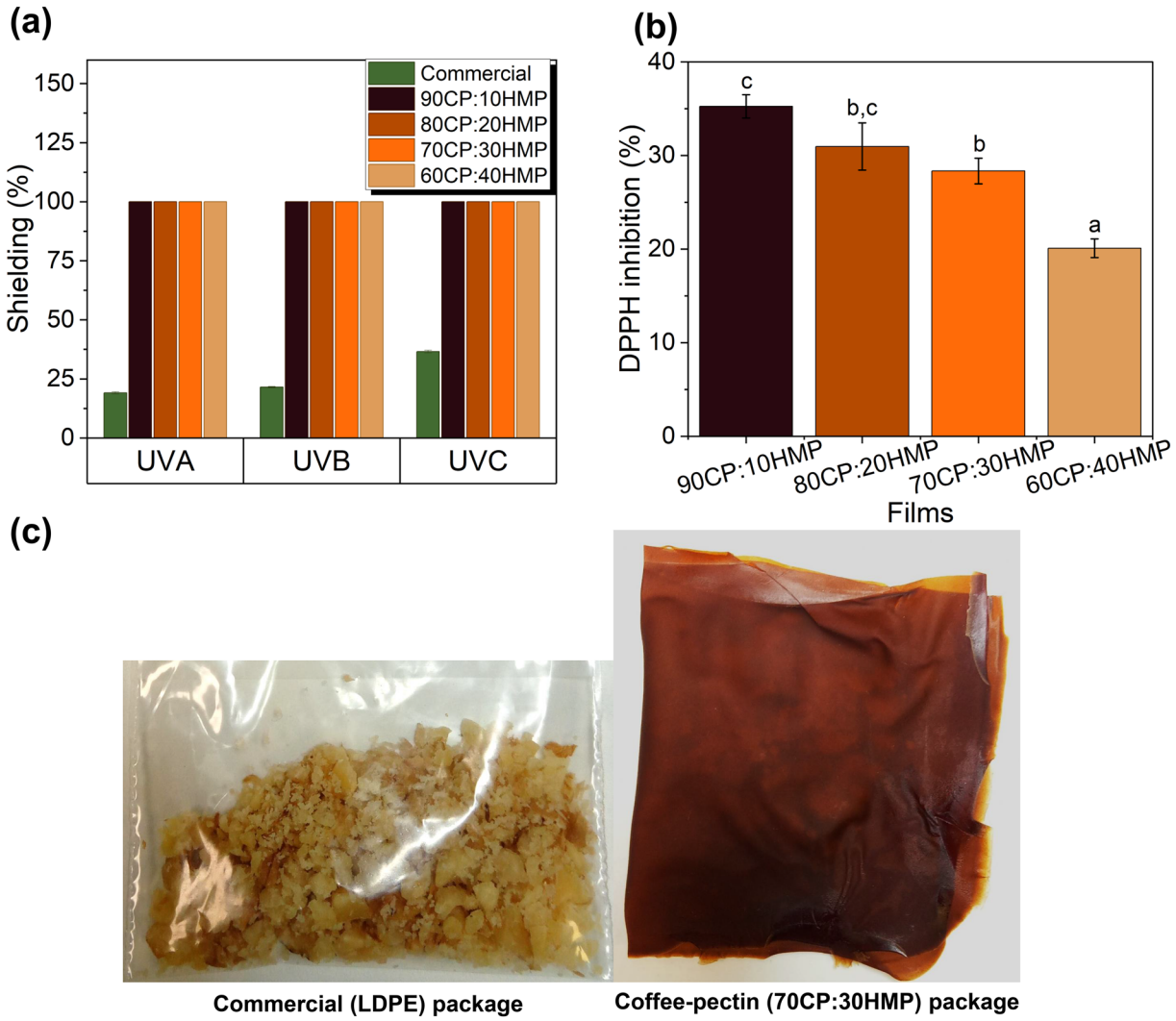

Fig. 5 (**a**) UV-shielding and (**b**) DPPH inhibition by the films developed in this work; (**c**) example of the packaging used in the oxidative stability test for the walnuts. In (**b**), treatments followed by at least one common letter are not significantly different from each other

contributing to their ability to mitigate oxidative processes that may compromise the stability and performance of light- and oxygen-sensitive products. Although the higher DPPH inhibition observed in films with higher coffee parchment content suggests a stronger contribution of biomass-derived compounds to the antioxidant response, this activity should not be attributed exclusively to the parchment fraction. Pectin itself may also exhibit measurable radical scavenging activity, which has been associated with structural features such as the presence of hydroxyl, carboxyl, and methoxy groups, as well as molecular-weight-related effects reported in the literature. Therefore, the antioxidant performance of the films is more appropriately interpreted as the result of the combined contribution of the parchment-derived compounds and the pectin matrix, with the relative contribution of the biomass becoming more evident as its proportion increases [110, 111].

To assess their UV-protective performance, these materials were tested to protect perishable items, such as walnuts, from photooxidation. To do this, ground walnuts were sealed in a conventional LDPE bag or between CP:HMP films that were thermally sealed, as shown in Fig. 5c.

Oils were extracted from the walnuts after the aging experiment, and the results, reported in Table 4 and Figure S5 (Supporting Information), show that oil preservation in walnuts differed by packaging type. Kernels stored in ordinary low-density polyethylene (LDPE) packaging exhibited a greater decrease in unsaturated bonds after seven days, correlated with a greater loss of proton intensity at olefinic, allylic, and bisallylic positions in ^{1}H-NMR (about 13.55–19.87%, Table 4). Oils extracted from the kernels stored in the active package showed minimal loss of intensity after seven days of UV irradiation instead (0.33–1.22%, Table 4).

Table 4 Losses of olefinic, bisallylic, and allylic proton intensities in walnut oils after UV exposure, as affected by packaging type (LDPE vs. active 70CP:30HMP film)

Packaging	% H* intensity loss		
	Day 7		
	Olefinic	**Bisallylic**	**Allylic**
Commercial	14.91^{B}	19.87^{B}	13.55^{B}
Active	0.33^{A}	1.22^{A}	0.81^{A}

*Calculated in relation to proton intensities obtained on day 0. Values followed by at least one common letter in the same column are not significantly different (Student, $p<0.05$)

For the oxidative stability assay, the 70CP:30HMP formulation was selected as test material because it provided a favorable balance between mechanical performance and functional properties. The comparison in Table 4 therefore reflects two distinct material behaviors: a conventional LDPE film, used as passive reference packaging, and a coffee parchment–pectin active film that combines complete UV-barrier capacity with intrinsic radical-scavenging activity. Under UV exposure, walnuts packed in LDPE exhibited substantially greater losses of olefinic, bisallylic, and allylic proton signals, whereas those packed in the 70CP:30HMP film showed only minimal changes. This result indicates that the developed active packaging was considerably more effective at mitigating photooxidative degradation under irradiation, primarily due to its light-shielding effect and, potentially, to the contribution of biomass-derived antioxidant compounds.

These results relate to the films' UV shielding properties, as shown in Fig. 5a. The presence of active molecules, such as phenolics, in the CP lends these films active properties, including UV-blocking and antioxidant capacity. These results suggest that active films could extend the preservation of walnut kernels and other nuts by retarding oxidation, likely due to the polyphenols present in the coffee biomass. These compounds can inhibit the photo-oxidation of lipids, retarding the formation and decomposition of hydroperoxides (ROOH), peroxides (ROOR), carboxylic compounds (RCOR), or other unsaturated lipid-oxygenated complexes [112].

Conclusions

Coffee parchment was identified as the most promising coffee processing by-product among the fractions evaluated and was successfully used in its whole form as the primary structural component of active bioplastics combined with high-methoxyl pectin.

The resulting films exhibited formulation-dependent mechanical behavior, allowing the material profile to be tailored by adjusting the parchment-to-pectin ratio, achieving complete UV-blocking capacity, and leveraging the radical-scavenging activity associated with intrinsic bioactive compounds from the biomass. In addition, the materials could be thermoformed into three-dimensional structures, indicating their potential for more complex packaging formats. The proof-of-concept study with walnuts demonstrated that the selected active film reduced the loss of unsaturated proton signals under UV exposure compared with conventional LDPE packaging, suggesting improved protection against photooxidative degradation. Overall, these findings highlight coffee parchment as an underexplored feedstock for whole-biomass valorization and support its potential use in active packaging applications for light-sensitive foods.

Supplementary Information The online version contains supplementary material available at https://doi.org/10.1007/s10924-026-03901-8.

Acknowledgements The authors gratefully acknowledge Wellington Marota Barbosa from the Federal Institute of Education, Science and Technology of Minas Gerais (IFSULDEMINAS, Campus Machado, MG, Brazil) for kindly providing the coffee by-products used in this study. We also thank Lara Marini for help with TGA measurements, Simone Lauciello from the Electron Microscopy Facility for help with SEM images, and Lea Pasquale and Lucca Ceseracciu from the Material Characterization Facility at the Fondazione Istituto Italiano di Tecnologia for help with XRD and tensile property measurements, respectively.

Author Contribution L.B.S.: Investigation; Formal Analysis; Writing—original draft. M.N.: Investigation; Formal analysis. R.S.: Investigation; Formal Analysis. G.P.: Conceptualization; Supervision; Writing—review & editing. C.G.O.: Supervision; Writing—review & editing. A.A.: Conceptualization. H.M.C.A.: Conceptualization; Funding acquisition; Project administration; Supervision; Writing—review & editing.

Funding The Article Processing Charge (APC) for the publication of this research was funded by the Coordenação de Aperfeiçoamento de Pessoal de Nível Superior - Brasil (CAPES) (ROR identifier: 00x0ma614). This work was supported by the Brazilian Coordination for the Improvement of Higher Education Personnel (CAPES, grant no. 88887.839474/2023–00), which supported the exchange program and international collaboration; by the Brazilian National Council for Scientific and Technological Development (CNPq, grant no. 406925/2022–4, INCT Circularity in Polymer Materials); and by the São Paulo Research Foundation (FAPESP, grants no. 2021/12071–6 and 2023/17111–1). Otoni and Azeredo also acknowledge Research Productivity Fellowships from CNPq (grant nos. 304753/2022–0 and 302950/2025–7, respectively).

Data Availability Data will be made available on request.

Declarations

Conflicts of Interest The authors declare no competing interests.

References

1. Organisation for Economic Co-operation and Development (2022) Plastic pollution is growing relentlessly as waste management and recycling fall short, says OECD. In: OECD. https://www.oecd.org/en/about/news/press-releases/2022/02/plastic-pollution-is-growing-relentlessly-as-waste-management-and-recycling-fall-short.html. Accessed 16 June 2025
2. Geyer R, Jambeck JR, Law KL (2017) Production, use, and fate of all plastics ever made. Sci Adv 3:25–29. https://doi.org/10.1126/sciadv.1700782
3. Walker TR, Fequet L (2023) Current trends of unsustainable plastic production and micro (nano) plastic pollution. TrAC, Trends Anal Chem 160:116984. https://doi.org/10.1016/j.trac.2023.116984
4. Otoni CG, Azeredo HMC, Mattos BD et al (2021) The food-materials nexus: next generation bioplastics and advanced materials from agri-food residues. Adv Mater. https://doi.org/10.1002/adma.202102520
5. Merino D, Quilez-Molina AI, Perotto G et al (2022) A second life for fruit and vegetable waste: a review on bioplastic films and coatings for potential food protection applications. Green Chem 24:4703–4727. https://doi.org/10.1039/D1GC03904K
6. Zhang D, Ahlivia EB, Bruce BB et al (2025) The road to re-use of spice by-products: exploring their bioactive compounds and significance in active packaging. Foods 14:2445. https://doi.org/10.3390/foods14142445
7. Cazón P, Mateus AR, Silva AS (2025) Advances in active packaging using natural biopolymers and fruit by-products for enhanced food preservation. Food Res Int 213:116439. https://doi.org/10.1016/j.foodres.2025.116439
8. Santos LB, Silva RD, Alonso JD et al (2023) Bioplastics from orange processing by-products by an ecoefficient hydrothermal approach. Food Packag Shelf Life 38:101114. https://doi.org/10.1016/j.fpsl.2023.101114
9. Silva RD, Pacheco TF, de Santi AD et al (2024) From bulk banana peels to active materials: slipping into bioplastic films with high UV-blocking and antioxidant properties. J Clean Prod 438:140709. https://doi.org/10.1016/j.jclepro.2024.140709
10. Perotto G, Ceseracciu L, Simonutti R et al (2018) Bioplastics from vegetable waste via an eco-friendly water-based process. Green Chem 20:894–902. https://doi.org/10.1039/c7gc03368k
11. Merino D, Simonutti R, Perotto G, Athanassiou A (2021) Direct transformation of industrial vegetable waste into bioplastic composites intended for agricultural mulch films. Green Chem 23:5956–5971. https://doi.org/10.1039/d1gc01316e
12. Perotto G, Simonutti R, Ceseracciu L et al (2020) Water-induced plasticization in vegetable-based bioplastic films a structural and thermo-mechanical study. Polymer. https://doi.org/10.1016/j.polymer.2020.122598
13. Merino D, Bertolacci L, Paul UC et al (2021) Avocado peels and seeds: processing strategies for the development of highly antioxidant bioplastic films. ACS Appl Mater Interfaces 13:38688–38699. https://doi.org/10.1021/acsami.1c09433
14. Quilez-Molina AI, Mazzon G, Athanassiou A, Perotto G (2022) A novel approach to fabricate edible and heat sealable bio-based films from vegetable biomass rich in pectin. Mater Today Commun 32:103871. https://doi.org/10.1016/j.mtcomm.2022.103871
15. Benítez JJ, Castillo PM, del Río JC et al (2018) Valorization of tomato processing by-products: fatty acid extraction and production of bio-based materials. Materials 11:1–13. https://doi.org/10.3390/ma11112211
16. Melo PEF, Silva APM, Marques FP et al (2019) Antioxidant films from mango kernel components. Food Hydrocolloids 95:487–495. https://doi.org/10.1016/j.foodhyd.2019.04.061
17. Oliveira TÍS, Rosa MF, Ridout MJ et al (2017) Bionanocomposite films based on polysaccharides from banana peels. Int J Biol Macromol 101:1–8. https://doi.org/10.1016/j.ijbiomac.2017.03.068
18. Pereira PHF, Waldron KW, Wilson DR et al (2017) Wheat straw hemicelluloses added with cellulose nanocrystals and citric acid. Effect on film physical properties. Carbohyd Polym 164:317–324. https://doi.org/10.1016/j.carbpol.2017.02.019
19. Wardana AA, Febrianto NA, Marcellino V et al (2025) Potency of coffee by-products as sustainable added material in bio/edible film development. Front Sustain Food Syst. https://doi.org/10.3389/fsufs.2025.1667255
20. Mottola S, Drago E, Montella F et al (2026) From spent coffee residues to sustainable packaging: zein-based active films produced via supercritical impregnation. J Supercrit Fluids 230:106865. https://doi.org/10.1016/j.supflu.2025.106865
21. Ilangovan M, Guna V, Hu C et al (2021) Dehulled coffee husk-based biocomposites for green building materials. J Thermoplast Compos Mater 34:1623–1638. https://doi.org/10.1177/0892705719876308
22. Leal H de A, Babetto AS, Bonse BC (2020) Properties of lignocellulosic composites of coffee husk filled polypropylene. AIP Conference Proceedings 2205:020072. https://doi.org/10.1063/1.5142987
23. Huang L, Mu B, Yi X et al (2018) Sustainable use of coffee husks for reinforcing polyethylene composites. J Polym Environ 26:48–58. https://doi.org/10.1007/s10924-016-0917-x
24. Das O, Kim NK, Hedenqvist MS et al (2018) An attempt to find a suitable biomass for biochar-based polypropylene biocomposites. Environ Manage 62:403–413. https://doi.org/10.1007/s00267-018-1033-6
25. Hidalgo-Salazar MÁ, Correa-Aguirre JP, Montalvo-Navarrete JM et al (2018) Recycled polypropylene-coffee husk and coir coconut biocomposites: morphological, mechanical, thermal and environmental studies. Thermosoftening Plastics. https://doi.org/10.5772/intechopen.81635
26. Yiga VA, Pagel S, Lubwama M et al (2020) Development of fiber-reinforced polypropylene with NaOH pretreated rice and coffee husks as fillers: mechanical and thermal properties. J Thermoplast Compos Mater 33:1269–1291. https://doi.org/10.1177/0892705718823255
27. Borghesi DC, Molina MF, Guerra MA, Campos MGN (2016) Biodegradation study of a novel poly-caprolactone-coffee husk composite film. Mat Res 19:752–758. https://doi.org/10.1590/1980-5373-MR-2015-0586
28. Lule ZC, Kim J (2021) Properties of economical and eco-friendly polybutylene adipate terephthalate composites loaded with surface treated coffee husk. Compos A Appl Sci Manuf 140:106154. https://doi.org/10.1016/j.compositesa.2020.106154
29. Ortiz-Barajas DL, Arévalo-Prada JA, Fenollar O et al (2020) Torrefaction of coffee husk flour for the development of injection-molded green composite pieces of polylactide with high sustainability. Appl Sci 10:6468. https://doi.org/10.3390/app10186468

30. Reis KC, Pereira L, Melo ICNA et al (2015) Particles of coffee wastes as reinforcement in polyhydroxybutyrate (PHB) based composites. Mat Res 18:546–552. https://doi.org/10.1590/1516-1439.318114
31. Sarasini F, Tirillò J, Zuorro A et al (2018) Recycling coffee silverskin in sustainable composites based on a poly(butylene adipate-co-terephthalate)/poly(3-hydroxybutyrate-co-3-hydroxyvalerate) matrix. Ind Crops Prod 118:311–320. https://doi.org/10.1016/j.indcrop.2018.03.070
32. Sung SH, Chang Y, Han J (2017) Development of polylactic acid nanocomposite films reinforced with cellulose nanocrystals derived from coffee silverskin. Carbohyd Polym 169:495–503. https://doi.org/10.1016/j.carbpol.2017.04.037
33. Valdespino-León M, Calderón-Domínguez G, De La Paz Salgado-Cruz M et al (2021) Biodegradable electrosprayed pectin films: an alternative to valorize coffee mucilage. Waste Biomass Valor 12:2477–2494. https://doi.org/10.1007/s12649-020-01194-z
34. Mirón-Mérida VA, Yáñez-Fernández J, Montañez-Barragán B, Barragán Huerta BE (2019) Valorization of coffee parchment waste (Coffea arabica) as a source of caffeine and phenolic compounds in antifungal gellan gum films. LWT 101:167–174. https://doi.org/10.1016/j.lwt.2018.11.013
35. Cacciotti I, Mori S, Cherubini V, Nanni F (2018) Eco-sustainable systems based on poly(lactic acid), diatomite and coffee grounds extract for food packaging. Int J Biol Macromol 112:567–575. https://doi.org/10.1016/j.ijbiomac.2018.02.018
36. Hernández-López G, Barrera-Necha LL, Bautista-Baños S et al (2025) Characterization of coffee waste-based biopolymer composite blends for packaging development. Foods 14:1991. https://doi.org/10.3390/foods14111991
37. Liu X, Sun H, Leng X (2023) Coffee silverskin cellulose-based composite film with natural pigments for food packaging: physicochemical and sensory abilities. Foods 12:2839. https://doi.org/10.3390/foods12152839
38. Hernández-Varela JD, Medina DI (2023) Revalorization of coffee residues: advances in the development of eco-friendly biobased potential food packaging. Polymers 15:2823. https://doi.org/10.3390/polym15132823
39. Petaloti A-I, Achilias DS (2024) The development of sustainable biocomposite materials based on poly(lactic acid) and silverskin, a coffee industry by-product, for food packaging applications. Sustainability 16:5075. https://doi.org/10.3390/su16125075
40. Iriondo-DeHond A, Aparicio García N, Fernandez-Gomez B et al (2019) Validation of coffee by-products as novel food ingredients. Innov Food Sci Emerg Technol 51:194–204. https://doi.org/10.1016/j.ifset.2018.06.010
41. Oliveira G, Passos CP, Ferreira P et al (2021) Coffee by-products and their suitability for developing active food packaging materials. Foods 10:683. https://doi.org/10.3390/foods10030683
42. Nzekoue FK, Angeloni S, Navarini L et al (2020) Coffee silverskin extracts: quantification of 30 bioactive compounds by a new HPLC-MS/MS method and evaluation of their antioxidant and antibacterial activities. Food Res Int 133:109128. https://doi.org/10.1016/j.foodres.2020.109128
43. Sudhakar DV, Maini SB (2000) Isolation and characterization of mango peel pectins. J Food Process Preserv 24:209–227. https://doi.org/10.1111/j.1745-4549.2000.tb00414.x
44. Gil DB, Bocourt EC, Maqueira YD (2006) Determinación de azúcares reductores totales en jugos mezclados de caña de azúcar utilizando el método del ácido 3,5 dinitrosalicílico. ICIDCA Sobre los Derivados de la Caña de Azúcar XL:45–50 ISSN: 0138–6204
45. Miller GL (1959) Use of dinitrosalicylic acid reagent for determination of reducing sugar. Anal Chem 31:426–428. https://doi.org/10.1021/ac60147a030
46. Singleton VL, Orthofer R, Lamuela-Raventós RM (1999) [14] Analysis of total phenols and other oxidation substrates and antioxidants by means of folin-ciocalteu reagent. In: Methods in Enzymology. Academic Press, pp 152–178 https://doi.org/10.1016/S0076-6879(99)99017-1
47. Silveira AC da, Kassuia YS, Domahovski RC, & Lazzarotto M. (2018). Método de DPPH adaptado: uma ferramenta para analisar atividade antioxidante de polpa de frutos da erva-mate de forma rápida e reprodutível [Adapted DPPH method: a tool for rapid and reproducible analysis of antioxidant activity in yerba mate fruit pulp]. Colombo: Embrapa Florestas. 11 p. (Embrapa Florestas. Technical Communication, 421). https://www.infoteca.cnptia.embrapa.br/handle/doc/1101294. Accessed on: May 29, 2026.
48. Rufino MD, Alves RE, de Brito ES, de Morais SM, Sampaio CD, Pérez-Jimenez J, Saura-Calixto FD. (2007). Metodologia científica: determinação da atividade antioxidante total em frutas pela captura do radical livre ABTS•+ [Scientific methodology: determination of total antioxidant activity in fruits by ABTS radical cation scavenging]. Fortaleza: Embrapa Agroindústria Tropical. 4 p. (Embrapa Agroindústria Tropical. Technical Communication, 128). https://www.infoteca.cnptia.embrapa.br/handle/doc/426954. Accessed on: May 29, 2026.
49. Juan-Polo A, Beltrán Sanahuja A, Monedero Prieto M et al (2023) Impact of UV-light irradiation on sensory properties, volatile, fatty acid, and tocopherol composition of peanuts (*Arachis hypogaea L.*). LWT 173:114247. https://doi.org/10.1016/j.lwt.2022.114247
50. Gao P, Liu R, Jin Q, Wang X (2019) Comparison of solvents for extraction of walnut oils: lipid yield, lipid compositions, minor-component content, and antioxidant capacity. LWT 110:346–352. https://doi.org/10.1016/j.lwt.2019.04.100
51. Liu Z, Vermillion K, Jin C et al (2021) NMR study on the oxidation of vegetable oils for assessing the antioxidant function of trehalose. Biocatal Agric Biotechnol 36:102134. https://doi.org/10.1016/j.bcab.2021.102134
52. Nolasco A, Squillante J, Velotto S et al (2022) Valorization of coffee industry wastes: comprehensive physicochemical characterization of coffee silverskin and multipurpose recycling applications. J Clean Prod 370:133520. https://doi.org/10.1016/j.jclepro.2022.133520
53. Cangussu LB, Melo JC, Franca AS, Oliveira LS (2021) Chemical Characterization of coffee husks, a by-product of coffea arabica production. Foods 10:3125. https://doi.org/10.3390/foods10123125
54. Cruz G, Braz CE, Ferreira SL, dos Santos AM, & Crnkovic PM. (2013). Physicochemical properties of Brazilian biomasses: potential applications as renewable energy source. In 22nd International Congress of Mechanical Engineering (pp. 10072–10084).
55. Dadi D, Beyene A, Simoens K et al (2017) Valorization of coffee by-products for bioethanol production using lignocellulosic yeast fermentation and pervaporation. Int J Environ Sci Technol 15:821–832. https://doi.org/10.1007/s13762-017-1440-x
56. Divyashri G, Tulsi NP, Murthy TPK et al (2024) Valorization of coffee bean processing waste for bioethanol production: comparison and evaluation of mass transfer effects in fermentations using free and encapsulated cells of saccharomyces cerevisiae. Bioprocess Biosyst Eng 47:169–179. https://doi.org/10.1007/s00449-023-02961-7
57. Gouvea BM, Torres C, Franca AS et al (2009) Feasibility of ethanol production from coffee husks. Biotechnol Lett 31:1315–1319. https://doi.org/10.1007/s10529-009-0023-4
58. Rebolledo Hernández MV, Cocotle-Ronzón Y, Hernández Martínez E, et al (2022) Propiedades fisicoquímicas, funcionales y de flujo de una harina de cáscara de café. CES 30. https://doi.org/10.30878/ces.v30n3a7
59. Shemekite F, Gómez-Brandón M, Franke-Whittle IH et al (2014) Coffee husk composting: an investigation of the process using molecular and non-molecular tools. Waste Manag 34:642–652. https://doi.org/10.1016/j.wasman.2013.11.010

60. Collazo-Bigliardi S, Ortega-Toro R, Chiralt A (2019) Improving properties of thermoplastic starch films by incorporating active extracts and cellulose fibres isolated from rice or coffee husk. Food Packag Shelf Life 22:100383. https://doi.org/10.1016/j.fpsl.2019.100383
61. Leão DP, Franca AS, Oliveira LS et al (2017) Physicochemical characterization, antioxidant capacity, total phenolic and proanthocyanidin content of flours prepared from pequi (*Caryocar brasilense* Camb.) fruit by-products. Food Chem 225:146–153. https://doi.org/10.1016/j.foodchem.2017.01.027
62. Clifford MN, Ramirez-Martinez JR (1991) Phenols and caffeine in wet-processed coffee beans and coffee pulp. Food Chem 40:35–42. https://doi.org/10.1016/0308-8146(91)90017-I
63. Ramirez-Martinez JR (1988) Phenolic compounds in coffee pulp: quantitative determination by HPLC. J Sci Food Agric 43:135–144. https://doi.org/10.1002/jsfa.2740430204
64. Ramirez-Coronel MA, Marnet N, Kolli VSK et al (2004) Characterization and estimation of proanthocyanidins and other phenolics in coffee pulp (Coffea arabica) by thiolysis−high-performance liquid chromatography. J Agric Food Chem 52:1344–1349. https://doi.org/10.1021/jf035208t
65. Prata ERBA, Oliveira LS (2007) Fresh coffee husks as potential sources of anthocyanins. LWT Food Sci Technol 40:1555–1560. https://doi.org/10.1016/j.lwt.2006.10.003
66. Mullen W, Nemzer B, Stalmach A et al (2013) Polyphenolic and hydroxycinnamate contents of whole coffee fruits from China, India, and Mexico. J Agric Food Chem 61:5298–5309. https://doi.org/10.1021/jf4003126
67. Machado M, Espírito Santo L, Machado S et al (2023) Bioactive potential and chemical composition of coffee by-products: from pulp to silverskin. Foods 12:2354. https://doi.org/10.3390/foods12122354
68. Jiménez-Zamora A, Pastoriza S, Rufián-Henares JA (2015) Revalorization of coffee by-products. prebiotic, antimicrobial and antioxidant properties. LWT Food Sci Technol 61:12–18. https://doi.org/10.1016/j.lwt.2014.11.031
69. Borrelli RC, Esposito F, Napolitano A et al (2004) Characterization of a new potential functional ingredient: coffee silverskin. J Agric Food Chem 52:1338–1343. https://doi.org/10.1021/jf034974x
70. Pourfarzad A, Mahdavian-Mehr H, Sedaghat N (2013) Coffee silverskin as a source of dietary fiber in bread-making: optimization of chemical treatment using response surface methodology. LWT Food Sci Technol 50:599–606. https://doi.org/10.1016/j.lwt.2012.08.001
71. Hijosa-Valsero M, Garita-Cambronero J, Paniagua-García AI, Díez-Antolínez R (2018) Biobutanol production from coffee silverskin. Microb Cell Fact 17:154. https://doi.org/10.1186/s12934-018-1002-z
72. Toschi TG, Cardenia V, Bonaga G et al (2014) Coffee silverskin: characterization, possible uses, and safety aspects. J Agric Food Chem 62:10836–10844. https://doi.org/10.1021/jf503200z
73. Alghooneh A, Mohammad Amini A, Behrouzian F, Razavi SMA (2017) Characterisation of cellulose from coffee silverskin. Int J Food Prop 20:2830–2843. https://doi.org/10.1080/10942912.2016.1253097
74. Zapateiro IN (2019) Propriedades funcionais da casca do café (Coffea arabica). Bachelor's Thesis, Universidade Tecnológica Federal do Paraná
75. Ávila PF, Martins M, Goldbeck R (2021) Enzymatic production of xylooligosaccharides from alkali-solubilized arabinoxylan from sugarcane straw and coffee husk. Bioenerg Res 14:739–751. https://doi.org/10.1007/s12155-020-10188-7
76. Bekalo SA, Reinhardt H-W (2010) Fibers of coffee husk and hulls for the production of particleboard. Mater Struct 43:1049–1060. https://doi.org/10.1617/s11527-009-9565-0
77. Nguyen DV, Duong CTT, Vu CNM et al (2023) Data on chemical composition of coffee husks and lignin microparticles as their extracted product. Data Brief 51:109781. https://doi.org/10.1016/j.dib.2023.109781
78. de Carvalho OF, Srinivas K, Helms GL et al (2018) Characterization of coffee (*Coffea arabica*) husk lignin and degradation products obtained after oxygen and alkali addition. Biores Technol 257:172–180. https://doi.org/10.1016/j.biortech.2018.01.041
79. Brum SS (2007) Caracterização e modificação química de resíduos sólidos do beneficiamento do café para produção de novos materiais. Master's thesis, Universidade Federal de Lavras
80. Campuzano F, Escobar DM, TL AM. (2024) Physicochemical characterization of coffee parchment of species coffea arabica variety castillo. Coffee Sci ISSN 1984-3909. 19:e192182–e192182. https://doi.org/10.25186/.v19i.2182
81. Ballesteros LF, Teixeira JA, Mussatto SI (2014) Chemical, functional, and structural properties of spent coffee grounds and coffee silverskin. Food Bioprocess Technol 7:3493–3503. https://doi.org/10.1007/s11947-014-1349-z
82. Mussatto SI, Machado EMS, Carneiro LM, Teixeira JA (2011) Sugars metabolism and ethanol production by different yeast strains from coffee industry wastes hydrolysates Sciencedirect. Appl Energy 92:6. https://doi.org/10.1016/j.apenergy.2011.08.020
83. Narita Y, Inouye K (2014) Review on utilization and composition of coffee silverskin. Food Res Int 61:16–22. https://doi.org/10.1016/j.foodres.2014.01.023
84. Franca A, Oliveira L (2009) Coffee processing solid wastes: Current uses and future perspectives. Agricultural Wastes 155–190 Nova Science Publishers, Inc. ISBN 978–1–60741–305–9
85. Narita Y, Inouye K (2012) High antioxidant activity of coffee silverskin extracts obtained by the treatment of coffee silverskin with subcritical water. Food Chem 135:943–949. https://doi.org/10.1016/j.foodchem.2012.05.078
86. Ribeiro EF, Luzia DMM, Jorge N (2019) Antioxidant compounds extraction from coffee husks: the influence of solvent type and ultrasound exposure time. Acta Sci Technol 41:e36451–e36451. https://doi.org/10.4025/actascitechnol.v41i2.36451
87. Zhang Z, Poojary MM, Choudhary A et al (2021) Ultrasound processing of coffee silver skin, brewer's spent grain and potato peel wastes for phenolic compounds and amino acids: a comparative study. J Food Sci Technol 58:2273–2282. https://doi.org/10.1007/s13197-020-04738-2
88. Puga H, Alves RC, Costa AS et al (2017) Multi-frequency multimode modulated technology as a clean, fast, and sustainable process to recover antioxidants from a coffee by-product. J Clean Prod 168:14–21. https://doi.org/10.1016/j.jclepro.2017.08.231
89. Wen L, Zhang Z, Sun D-W et al (2020) Combination of emerging technologies for the extraction of bioactive compounds. Crit Rev Food Sci Nutr 60:1826–1841. https://doi.org/10.1080/10408398.2019.1602823
90. Guglielmetti A, D'ignoti V, Ghirardello D et al (2017) Optimisation of ultrasound and microwave assisted extraction of caffeoylquinic acids and caffeine from coffee silverskin using response surface methodology. Ital J Food Sci. https://doi.org/10.14674/IJFS-727
91. Barbosa-Pereira L, Guglielmetti A, Zeppa G (2018) Pulsed electric field assisted extraction of bioactive compounds from cocoa bean shell and coffee silverskin. Food Bioprocess Technol 11:818–835. https://doi.org/10.1007/s11947-017-2045-6
92. Zengin G, Sinan KI, Mahomoodally MF et al (2020) Chemical composition, antioxidant and enzyme inhibitory properties of different extracts obtained from spent coffee ground and coffee silverskin. Foods 9:713. https://doi.org/10.3390/foods9060713
93. Bessada SMF, Alves RC, Costa ASG et al (2018) *Coffea canephora* silverskin from different geographical origins: A

comparative study. Sci Total Environ 645:1021–1028. https://doi.org/10.1016/j.scitotenv.2018.07.201
94. Yang H, Yan R, Chen H et al (2007) Characteristics of hemicellulose, cellulose and lignin pyrolysis. Fuel 86:1781–1788. https://doi.org/10.1016/j.fuel.2006.12.013
95. Reis R, Tienne L, Souza D et al (2020) Characterization of coffee parchment and innovative steam explosion treatment to obtain microfibrillated cellulose as potential composite reinforcement. J Mater Res Technol. https://doi.org/10.1016/j.jmrt.2020.05.099
96. Lima M, Borsali R (2004) Rodlike cellulose microcrystals: structure, properties, and applications. Macromol Rapid Commun 25:771–787. https://doi.org/10.1002/marc.200300268
97. Reichembach LH, Guerrero P, de Oliveira Petkowicz CL, de la Caba K (2024) Valorization of pectins from coffee wastes for the development of pectin-chitosan films. Carbohyd Polym 334:122057. https://doi.org/10.1016/j.carbpol.2024.122057
98. Konstantinidis N, Franke H, Schwarz S, Lachenmeier DW (2023) Risk assessment of trigonelline in coffee and coffee by-products. Molecules 28:3460. https://doi.org/10.3390/molecules28083460
99. Reis N, Franca AS, Oliveira LS (2013) Discrimination between roasted coffee, roasted corn and coffee husks by diffuse reflectance infrared fourier transform spectroscopy. LWT Food Sci Technol 50:715–722. https://doi.org/10.1016/j.lwt.2012.07.016
100. Szymanska-Chargot M, Chylinska M, Kruk B, Zdunek A (2014) Combining FT-IR spectroscopy and multivariate analysis for qualitative and quantitative analysis of the cell wall composition changes during apples development. Carbohydr Polym. https://doi.org/10.1016/j.carbpol.2014.08.039
101. Shankar S, Tanomrod N, Rawdkuen S, Rhim J-W (2016) Preparation of pectin/silver nanoparticles composite films with UV-light barrier and properties. Int J Biol Macromol 92:842–849. https://doi.org/10.1016/j.ijbiomac.2016.07.107
102. Yaradoddi JS, Banapurmath NR, Ganachari SV et al (2021) Bio-based material from fruit waste of orange peel for industrial applications. J Mater Res Technol. https://doi.org/10.1016/j.jmrt.2021.09.016
103. Siripatrawan U, Harte BR (2010) Physical properties and antioxidant activity of an active film from chitosan incorporated with green tea extract. Food Hydrocoll 24:770–775. https://doi.org/10.1016/j.foodhyd.2010.04.003
104. Mendes JF, Martins JT, Manrich A et al (2019) Development and physical-chemical properties of pectin film reinforced with spent coffee grounds by continuous *casting*. Carbohyd Polym 210:92–99. https://doi.org/10.1016/j.carbpol.2019.01.058
105. Jantrawut P, Chaiwarit T, Jantanasakulwong K et al (2017) Effect of plasticizer type on tensile property and in vitro indomethacin release of thin films based on low-methoxyl pectin. Polymers (Basel) 9:289. https://doi.org/10.3390/polym9070289
106. Asfaw WA, Tafa KD, Satheesh N (2023) Optimization of citron peel pectin and glycerol concentration in the production of edible film using response surface methodology. Heliyon 9:e13724. https://doi.org/10.1016/j.heliyon.2023.e13724
107. Ozbayoglu G (2018) 3.19 Energy production from coal. Comp Energy Syst 3–5:788–821. https://doi.org/10.1016/B978-0-12-809597-3.00341-2
108. Ezati P, Khan A, Priyadarshi R et al (2023) Biopolymer-based UV protection functional films for food packaging. Food Hydrocoll. https://doi.org/10.1016/j.foodhyd.2023.108771
109. Ballesteros LF, Cerqueira MA, Teixeira JA, Mussatto SI (2018) Production and physicochemical properties of carboxymethyl cellulose films enriched with spent coffee grounds polysaccharides. Int J Biol Macromol 106:647–655. https://doi.org/10.1016/j.ijbiomac.2017.08.060
110. Liu N, Yang W, Li X et al (2022) Comparison of characterization and antioxidant activity of different citrus peel pectins. Food Chem 386:132683. https://doi.org/10.1016/j.foodchem.2022.132683
111. Roy S, Priyadarshi R, Łopusiewicz Ł et al (2023) Recent progress in pectin extraction, characterization, and pectin-based films for active food packaging applications: a review. Int J Biol Macromol 239:124248. https://doi.org/10.1016/j.ijbiomac.2023.124248
112. Frankel EN (2012) Chapter 3 - Photooxidation of unsaturated fats. In: Frankel EN (ed) Lipid Oxidation (Second Edition). Woodhead Publishing, pp 51–66 https://doi.org/10.1533/9780857097927.51.